Journal of Applied Polymer Science

Chitin Nanocrystal Reinforced Wet-Spun Chitosan Fibers

Weixia Yan,[1,2] Libin Shen,[1] Yali Ji,[1] Qing Yang,[1] Xinyuan Shen[1]

[1]State Key Laboratory for Modification of Chemical Fibers and Polymer Materials, College of Material Science and Engineering, Donghua University, Shanghai 201620, China

[2]Analysis and Testing Center, Donghua University, Shanghai 201620, China

Correspondence to: Y. Ji (E-mail: jiyali@dhu.edu.cn)

ABSTRACT: Chitosan (CS) has been extensively studied and found wide applications in the field of biomedicine because of its favorable biological properties. Normal CS fibers are manufactured either by wet-spinning or by dry-jet wet-spinning. However, the poor tensile strength of CS fibers raises much concern. The present study uses chitin nanocrystal (ChiNC), a stiff rod-like nanofiller, to enhance the mechanical properties of wet-spun CS fibers. Owing to the good compatibility between CS and ChiNC, the nanoparticles are well distributed in the CS matrix. When the ChiNCs loading is 5 wt %, the optimal mechanical properties of CS fibers are obtained, and the peak stress is 2.2 cN/dtex and modulus is 145.6 cN/dtex, which are increased by 57% and 84.5%, respectively, compared to that of nonfilled CS fibers under the same processing condition. © 2014 Wiley Periodicals, Inc. J. Appl. Polym. Sci. **2014**, *131*, 40852.

KEYWORDS: fibers; mechanical properties; nanoparticles; nanowires and nanocrystals; polysaccharides

Received 29 January 2014; accepted 12 April 2014

DOI: 10.1002/app.40852

INTRODUCTION

Chitin/Chitosan (CS) is the second most abundant biopolymer next to cellulose and possesses many favorable properties such as nontoxicity, biocompatibility, and biodegradability.[1] Dissolved in aqueous acid solution as spinning dope and aqueous alkaline solution as coagulation bath, CS can be wet-spun[2–4] or dry-jet wet-spun to fibers.[5] CS fibers have been found wide clinical applications such as wound dressing,[6–9] surgical suture,[10,11] and tissue scaffold.[12–14] Also, a good antibacterial activity of CS makes CS fiber an ideal candidate for manufacturing underwear in the textile field.[15–17] However, the tensile strength of present CS fibers is undesirable, and many studies were performed to improve the mechanical properties of CS fibers.

Agboh and Qin[3] took several physical treatments to improve the Young's modulus and tenacity of wet-spun CS fibers, including increasing the draw ratio of as-spun fibers in the washing and drawing baths, enhancing the spinneret draw, or performing the heat treatment toward as-spun fibers. Knaul et al.[18] utilized several posttreatment methods to reinforce CS fibers, such as using direct and radiant heat, forced air, or some chemical drying agents of acetone, isopropanol or methanol to treat as-spun CS fibers. Moreover, epichlorohydrin,[19] glyoxal,[20] and glutaraldehyde[21] were used as cross-linking agents to chemically strengthen CS fibers. In recent study, Li et al.[22] used ionic liquid as spinning dope solution for preparing CS fibers and found the mechanical properties of CS fibers were highly improved. In addition, the nanocomposite method of loading the nanoparitcles such as polyhedral oligomeric silsesquioxane and single-walled carbon nanotubes into the CS spinning dope to wet-spin was also proved to be able to increase CS fibers' strength.[23]

However, compared to the inorganic nanofillers, chitin nanocrystal (ChiNC, otherwise called nanowhiskers or nanofibrils), an emerging, novel, rod-like nanofiller, extracted from acid-treatment of chitin, possesses many advantages of nanodimension, high surface area, low density, high modulus, and ideal reinforcing ability to polymeric structures, as well as good biocompatibility and biodegradability. ChiNCs-based nanocomposites have been extensively explored especially in the field of biomedical materials.[24] Many polymers were used as matrices, such as polyvinyl alcohol, soy protein isolate, CS, gelatin, alginate, cellulose, silk fibroin, and waterborne polyurethane via aqueous blending, and polycaprolactone and poly(S-co-BuA) via latex blending. All of them exhibited the prominently enhanced mechanical properties by loading ChiNCs.[25–34] But to our knowledge, ChiNCs reinforced CS fiber had not been explored. So this study used ChiNCs as reinforcing nanofiller to wet-spin CS/ChiNC nanocomposite fibers, expecting to obtain high strength CS fibers.

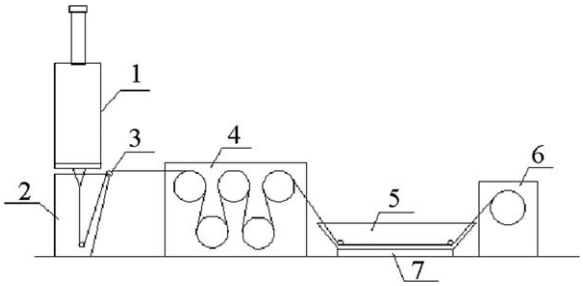

Figure 1. Schematic of homemade setup of wet-spinning. (1-storage barrel; 2-coagulation bath; 3-filament guide; 4-guide roller; 5-washing and drawing bath; 6-take up roller; and 7-heating board).

EXPERIMENTAL

Preparation of ChiNC

ChiNC suspension was prepared according to our previous report.[35] Briefly, chitin flakes were hydrolyzed in 3*M* HCl under stirring and refluxing for 6 h. The ratio of the 3*M* HCl solution to chitin was 30 cm^3 g^{-1}. The residue was collected after centrifugation and treated twice with 3*M* HCl. Then, the residue was washed with deionized water for three times by centrifugating and decanting the supernatant. The obtained suspension was further dialyzed in deionized water at room temperature for 3 days, followed by ultrasonic treatment and subsequent filtration to remove residual aggregates. Finally, the suspension was lyophilized to obtain light brown powders. The yield was about 55%.

Wet-Spinning of CS/ChiNC Nanocomposite Fibers

A desirable amount of CS powders were dissolved in 3 wt % acetic acid aqueous solution by constant stirring at 30°C. The CS concentration was maintained at 3 wt % in all samples. ChiNCs powders were redispersed in deionized water via ultrasonication, and then mixed with the CS solution by controlling the mass ratio of ChiNC to CS at 0, 2.5, 5, and 10 wt %. The mixtures were kept stirring for 10–12 h, and then vacuum filtered with a 300 mesh sieve, degassed under vacuum, and finally sealed up for wet-spinning. A homemade spinning setup was used for wet-spinning as shown in Figure 1. The spinning solutions were extruded through a stainless steel six-hole spinneret into a coagulation bath consisting of NaOH–Na_2SO_4 aqueous solution (NaOH: 20 g L^{-1}; Na_2SO_4: 100 g L^{-1}). The fibers obtained from the coagulation bath were washed in water and stretched at a suitable draw ratio in a washing–drawing bath at 70°C. The draw ratio was controlled by varying the speed of guide roller relative to the speed of take-up roller.

Measurement and Characterization

The morphology and dispersibility of ChiNCs were evaluated via transmission electron microscopy (TEM). A drop of diluted suspension was cast onto a carbon coated copper grid, slowly evaporated at room temperature, and then observed on a 2100F TEM (JEOL, Japan). A Leica DM750P polarized optical microscope was used to evaluate the dispersivity of ChiNC in the CS acetic acid aqueous solution.

The surface and cross-section morphologies of fibers were observed on SU8010 field emission scanning electron microscope (Hitachi, Japan). The fiber bundle was embedded into epoxy resin, and then cryo-fractured in liquid nitrogen to obtain cross-section of individual fiber.

Fourier transform infrared spectra (FTIR) were measured on a Nicolet 670 Nexus FTIR spectrometer over a wavenumber range of 400–4000 cm^{-1} at 4 cm^{-1} resolution via accumulation of 32 scans. The fibers were cut into crumbs and pressed with KBr powder before measurement. The obtained spectra were normalized.

Wide angle X-ray diffraction (WAXD) patterns were recorded on a D/Max-2550 PC diffractometer (Rigaku, Japan) at room temperature operated at 40 kV and 200 mA. The scan speed was 3 min^{-1} in the range of 5–50°. The fibers were cut into crumbs. The relative crystallinity was calculated using the Jade 6.5 software.

The filament number of CS fibers was measured on a homemade XD-1 fiber fineness tester. The mechanical properties of CS fibers were tested on a homemade XQ-1C tensile strength tester with a crosshead speed of 10 mm min^{-1} and clamp distance of 20 mm. The results of tensile modulus, stress, and break at strain were the average of 20 tests.

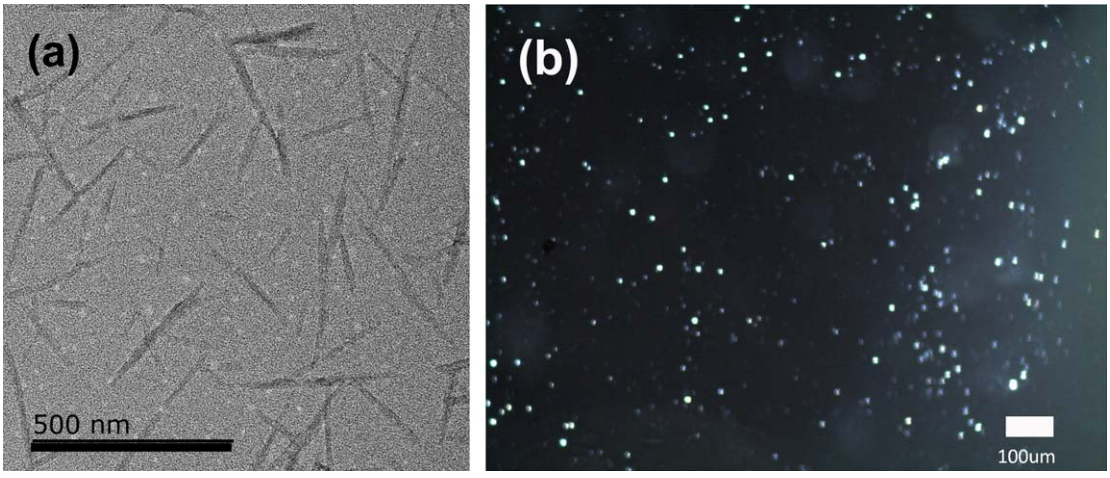

Figure 2. (a) Transmission electron micrograph of a dilute suspension of ChiNC (scale bar = 500 nm); (b) cross-polarizing optical microphotographs of ChiNC dispersed in CS solution (scale bar = 100 μm). [Color figure can be viewed in the online issue, which is available at wileyonlinelibrary.com.]

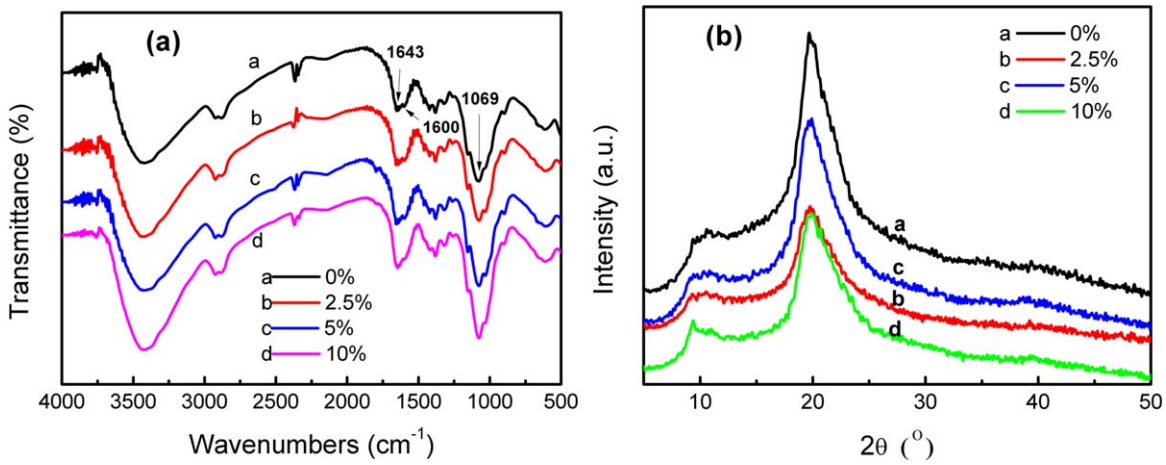

Figure 3. (a) FTIR spectra and (b) WAXD patterns of CS/ChiNC nanocomposite fibers. [Color figure can be viewed in the online issue, which is available at wileyonlinelibrary.com.]

Table I. The Relative Crystallinity of CS/ChiNC Fibers

ChiNC load (wt %)	Relative crystallinity (%)
0	33.2
2.5	24
5	30
10	25.3

Thermogravimetric analysis (TGA) was carried on a TG 209 thermal analyzer (Netzsch) to investigate the thermal stability of the fibers. The scanning range was 30–600°C with a heating rate of 10°C min^{-1} under a nitrogen atmosphere.

RESULTS AND DISCUSSIONS

Dimensions and Dispersion of ChiNCs

Figure 2a shows the transmission electron micrograph of a dilute ChiNC aqueous suspension obtained by redispersing ChiNC powders into water. The ChiNCs were individually dispersed and the estimated average width, length, and aspect ratio L/d (L being the length and d being the width) was 20 nm, 300 nm, and 15, respectively. Figure 2b depicts the cross-polarizing optical micrograph of the CS/ChiNC (mass ratio, 1 : 0.1) mixture in 3% acetic acid aqueous solution. There appear a large number of uniformly distributive bright dots representing the birefringence of ChiNCs, indicating ChiNCs were uniformly dispersed in the CS solution.

Structure and Compatibility of Nanocomposite Fibers

The FTIR spectra of wet-spun fibers are shown in Figure 3a. The characteristic absorption peaks of CS at 1643 cm^{-1} (amide I), 1600 cm^{-1} (—NH_2), and 1069 cm^{-1} (C—O) were present in all the samples. Compared to the neat CS fiber, the bands around 3400 cm^{-1} (assigned to the stretching vibration of —OH) became broader with the addition of ChiNCs, indicating the strong hydrogen bonds between the CS matrix and the ChiNC nanofiller occurred.

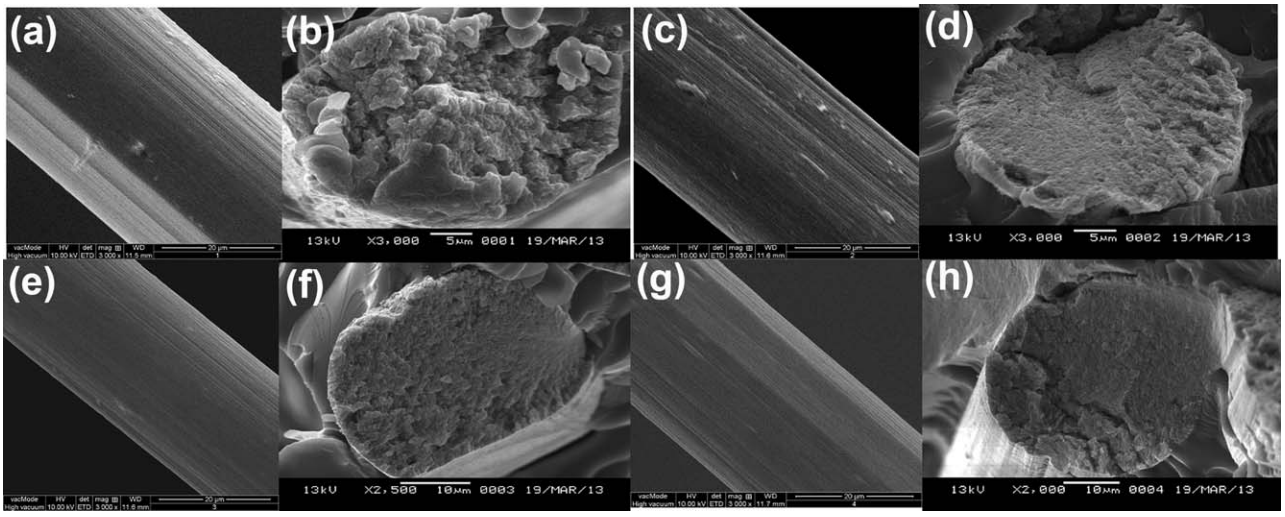

Figure 4. The morphologies of outer surface and cross-section of wet-spun fibers with the ChiNC loading of (a) 0 wt %, surface; (b) 0 wt %, section; (c) 2.5 wt %, surface; (d) 2.5 wt %, section; (e) 5 wt %, surface; (f) 5 wt %, section; (g) 10 wt %, surface; and (h)10 wt %, section.

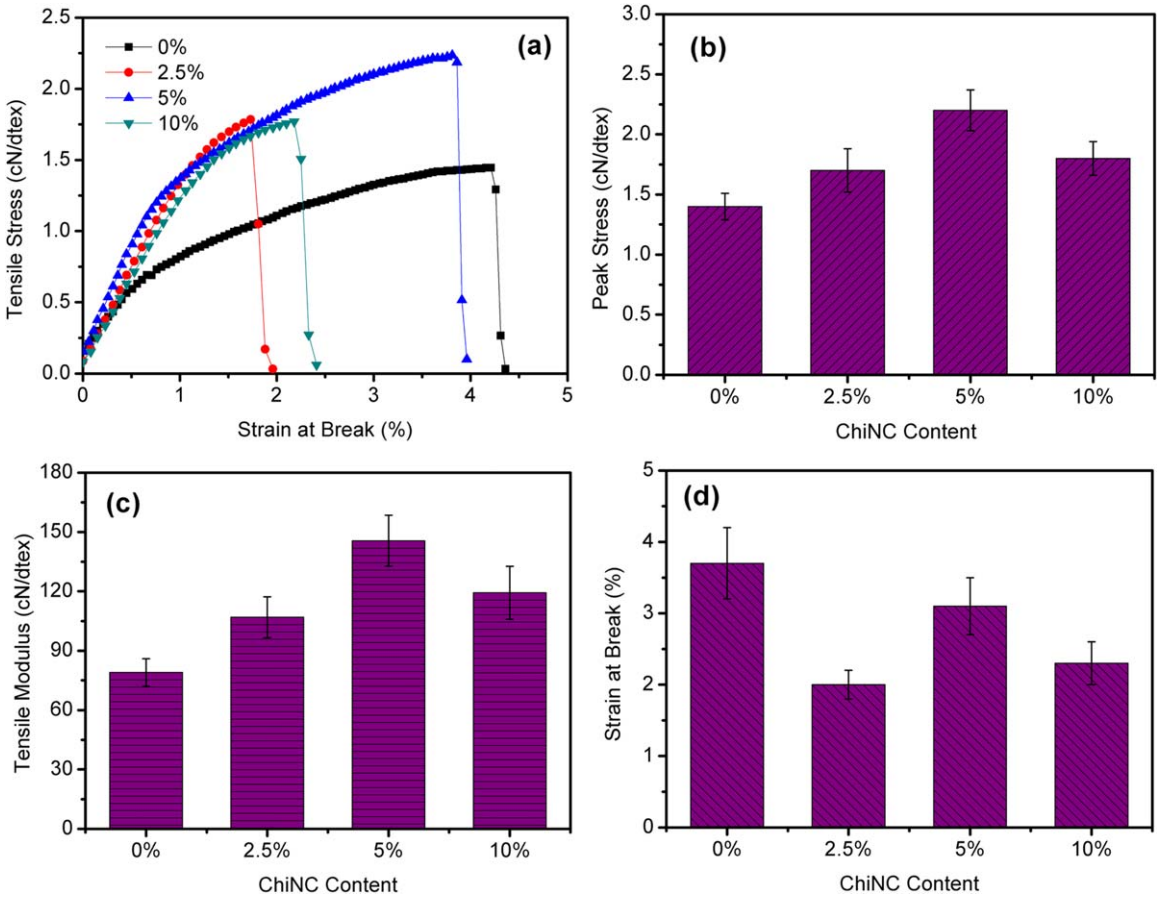

Figure 5. Uniaxial tensile tests of CS and CS/ChiNC fibers obtained at 1.5 draw ratio. The strain–stress curves close to the average tensile stress from 9 to 10 tests were selected to display here (a); the data of peak stress (b), tensile modulus (c), and strain at break (d) were the average of 9–10 tests. [Color figure can be viewed in the online issue, which is available at wileyonlinelibrary.com.]

WAXD spectra from 5° to 50° in Figure 3b exhibit the crystal peaks of the neat CS fiber and the nanocomposite fibers. The CS fiber displayed characteristic diffraction crystalline peaks at 2θ of 10.8 and 19.9°. These peaks still existed but the intensities weakened in the CS/ChiNC fibers. In addition, the diffraction peaks of ChiNC at 2θ of 9.6° appeared with the increase of ChiNC loading. The results revealed that the ChiNC existed in the nanocomposite fibers, and strong interaction between ChiNC and CS appeared here. The relative crystallinity of CS in all fibers was calculated by Jade 6.5 software, and the results are displayed in Table I. With the loading of ChiNCs, the relative crystallinity of CS decreased, possibly due to the interaction between ChiNCs and CS, which hindered the movement of CS macromolecular chains.

Table II. The Mechanical Properties of 5 wt % CS/ChiNC Fibers Obtained at Various Draw Ratio[a]

Draw ratio	Filament number (dtex)	Tensile stress (cN/dtex)	Strain at break (%)	Tensile modulus (cN/dtex)
1.1	11.6	1.42	8.64	70.22
1.2	10.6	1.58	4.51	76.73
1.3	9.41	1.77	4.02	108.1
1.4	9.30	2.04	4.08	167.4
1.5	9.13	2.21	3.14	145.6

[a]The data of filament number, tensile stress, modulus, and strain at break were the average of 9–10 tests.

The CS/ChiNC fibers were obtained by wet-spinning at the draw ratio of 1.5. Figure 4 shows the morphologies of outer surface and corss-section of wet-spun fibers with various ChiNC loading. There were no appreciable differences in outer surface among them, and all the fibers contained striations that were attributed to shrinking during drying. However, the fiber without ChiNC loading, had a more coarse and loose cross-section structure. Instead, the addition of ChiNC into CS caused a more smooth and compact cross-section structure. Thus, the loading of ChiNCs into CS could improve the morphology of CS fibers.

Mechanical Properties of Fibers

Figure 5 shows the mechanical properties of the CS and CS/ChiNC fibers. With the increase of ChiNC loading, the tensile peak stress was improved from 1.41 cN/dtex (neat CS fiber) to 2.21 cN/dtex (5 wt % CS/ChiNC fiber), the tensile modulus also highly increased compared to the neat CS fiber (78.98 cN/dtex), the highest being 145.6 cN/dtex (5 wt % CS/ChiNC

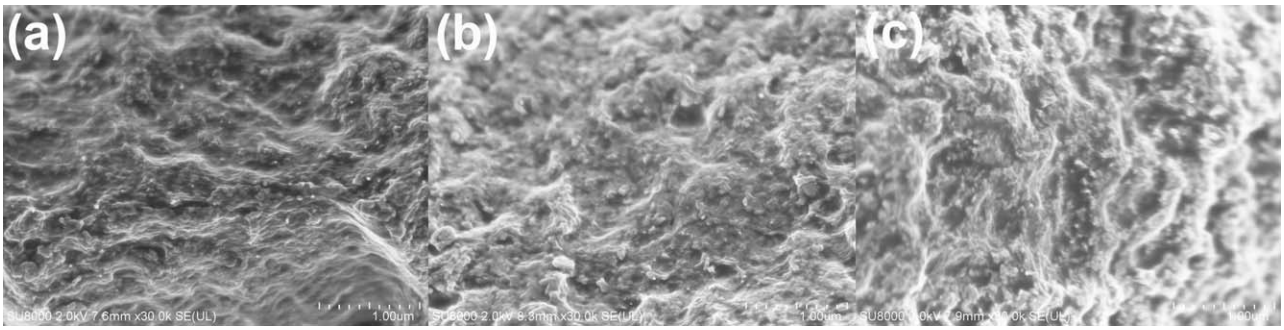

Figure 6. The cross-section of 5 wt % CS/ChiNC fibers obtained at the draw ratio of (a) 1.1; (b) 1.3; and (c) 1.5.

fiber), however, the strain at break decreased slightly to the range of 1.95–3.14% compared to the neat CS fiber (3.66%). Thus, in consideration of our aim, the loading of 5 wt % ChiNC into CS was optimal, of which the tensile strength increased by 57%, tensile modulus increased by 87%, whereas, strain at break only lost by 14% in comparison to the neat CS fiber.

The effects of draw ratio on the mechanical properties of wet-spun fibers are shown in Table II. Taking 5 wt % CS/ChiNC fiber as example, with the increase of the draw ratio, the filament number decreased, the tensile stress and modulus both increased, and the strain at break decreased. The increase in mechanical properties with draw ratio was due to the increase in molecular chain orientation caused by stretching.[36] The decrease in strain at break suggested that a plastic deformation had been imposed on the fiber and made the fibers more brittle.[36] Thus, the increase of draw ratio favored the enhancement of the mechanical properties of fibers, but the fiber would be broken when the draw ratio exceeding 1.5.

Figure 6 shows the magnified cross-section micrographs of 5 wt % CS/ChiNC fibers at various draw ratio. The bright dots were designated as ChiNCs, which were uniformly distributed in the CS matrix. We had thought the draw ratio would affect the ChiNCs' orientation in the fibers, and the higher draw ratio would produce the better orientation of ChiNCs along fiber axis, that is, more bright dots should appear. But from Figure 6, it did not show any visible changes with draw ratio. Even so, it could be concluded that the ChiNCs and CS had a good compatibility so that ChiNCs could be homogeneously distributed in the CS matrix and enhance the CS fibers.

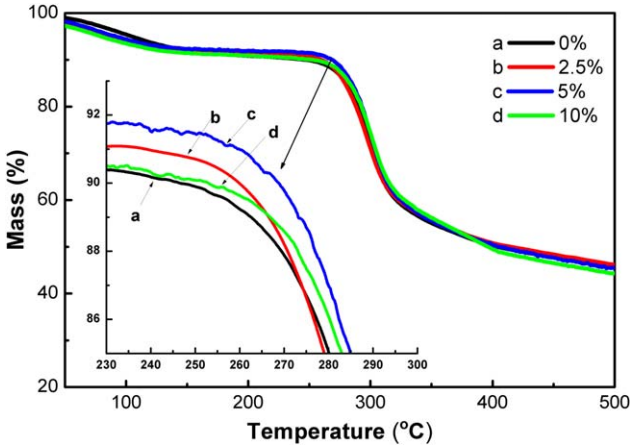

Figure 7. TGA of CS/ChiNC fibers. [Color figure can be viewed in the online issue, which is available at wileyonlinelibrary.com.]

Thermal Properties of Fibers

The TGA thermograms shown in Figure 7 indicated the loading of ChiNCs did not have visible influence on the thermal stability of CS fiber, although ChiNCs possess higher thermal decomposition temperature than that of CS.

CONCLUSIONS

In summary, the ChiNC can well disperse in the CS acetic acid aqueous solution. Through wet-spinning, the CS/ChiNC nanocomposite fibers with improved mechanical properties have been successfully fabricated. The formation of hydrogen bonds between CS and ChiNC conferred good compatibility between the filler and the matrix, leading to the homogeneous distribution of ChiNC in the CS matrix. With the increase of ChiNC loading, the tensile strength and modulus increased. The optimal loading was 5 wt %, of which the peak stress was 2.2 cN/dtex and the modulus was 145.6 cN/dtex, which were increased by 57.0% and 84.5%, respectively, compared to that of neat CS fibers. Further increasing the ChiNC loading would damage the mechanical properties. The increase of draw ratio favored the enhancement of the mechanical properties of nanocomposite fibers, and the ultimate draw ratio was 1.5. In addition, the loading of ChiNCs did not have appreciable influence on the thermal stability of CS fiber.

ACKNOWLEDGMENTS

This work was supported by the program from the National Natural Science Foundation of China (Grant No. 51303024), the Natural Science Foundation of Shanghai (Grant No. 10ZR1400900), and the Fundamental Research Funds for the Central Universities.

REFERENCES

1. Dash, M.; Chiellini, F.; Ottenbrite, R. M.; Chiellini, E. *Prog. Polym. Sci.* **2011**, *36*, 981.
2. East, G. C.; Qin, Y. *J. Appl. Polym. Sci.* **1993**, *50*, 1773.
3. Agboh, O. C.; Qin, Y. *Polym. Adv. Technol.* **1997**, *8*, 355.

4. Knaul, J. Z.; Hudson, S. M.; Creber, K. A. M. *J. Appl. Polym. Sci.* **1999**, *72*, 1721.
5. Yang, Q.; Liang, B.; Shen, X.; Tan, Z.; Zhang, C. *Huagong Jinzhan* **2005**, *24*, 643.
6. Rajendran, S.; Anand, S. C. *Indian J. Fiber Text. Res.* **2006**, *31*, 215.
7. Muzzarelli, R. A. A.; Morganti, P.; Morganti, G.; Palombo, P.; Palombo, M.; Biagini, G. *Carbohydr. Polym.* **2007**, *70*, 274.
8. Xie, H.; Khajanchee, Y. S.; Teach, J. S.; Shaffer, B. S. *J. Biomed. Mater. Res. B: Appl. Biomater.* **2008**, *85*, 267.
9. Yudanova, T. N.; Reshetov, I. V. *Pharm. Chem. J.* **2006**, *40*, 85.
10. Austin, P. R.; Brine, C. J.; Castle, J. E.; Zikakis, J. P. *Science* **1981**, *212*, 749.
11. Khor, E.; Lim, L. Y. *Biomaterials* **2003**, *24*, 2339.
12. Yu, Z.; Xu, H. H. K. *J. Biomed. Mater. Res. A* **2005**, *75*, 832.
13. Li, X.; Feng, Q.; Jiao, Y.; Cui, F. *Polym. Int.* **2005**, *54*, 1034.
14. Tuzlakoglu, K.; Alves, C. M.; Mano, J. F.; Reis, R. L. *Macromol. Biosci.* **2004**, *4*, 811.
15. Qin, Y.; Zhu, C.; Chen, J.; Zhong, J. *J. Appl. Polym. Sci.* **2007**, *104*, 3622.
16. Qin, Y.; Zhu, C.; Chen, J.; Chen, Y.; Zhong, J. *J. Appl. Polym. Sci.* **2006**, *101*, 766.
17. Shin, Y.; Yoo, D. I.; Min, K. *J. Appl. Polym. Sci.* **1999**, *74*, 2911.
18. Knaul, J.; Hooper, M.; Chanyi C.; Creber, K. A. M. *J. Appl. Polym. Sci.* **1998**, *69*, 1435.
19. Lee, S.; Park, S.; Kim, Y. *Carbohydr. Polym.* **2007**, *70*, 53.
20. Yang, Q.; Dou, F.; Liang, B.; Shen, Q. *Carbohydr. Polym.* **2005**, *59*, 205.
21. Knaul, J. Z.; Hudson, S. M.; Creber K. A. M. *J. Polym. Sci.* **1999**, *37*, 1079.
22. Li, L.; Yuan, B.; Liu, S.; Yu, S.; Xie, C.; Liu, F.; Guo, X.; Pei, L.; Zhang, B. *J. Mater. Chem.* **2012**, *22*, 8585.
23. Chen, J.; Loo, L. S.; Wang, K. *Carbohydr. Polym.* **2011**, *86*, 1151.
24. Dufresne, A. *Can. J. Chem.* **2008**, *86*, 484.
25. Uddin, A. J.; Fujie, M.; Sembo, S.; Gotoh, Y. *Carbohydr. Polym.* **2012**, *87*, 799.
26. Lu, Y.; Weng, L.; Zhang, L. *Biomacromolecules* **2004**, *5*, 1046.
27. Li, X.; Li, X.; Ke, B.; Shi, X.; Du, Y. *Carbohydr. Polym.* **2011**, *85*, 747.
28. Hariraksapitak, P.; Supaphol, P. *J. Appl. Polym. Sci.* **2010**, *117*, 3406.
29. Watthanaphanit, A.; Supaphol, P.; Tamura, H.; Tokura, S.; Rujiravanit, R. *J. Appl. Polym. Sci.* **2008**, *110*, 890.
30. Huang, Y.; Zhang, L.; Yang, J.; Zhang, X.; Xu, M. *Macromol. Mater. Eng.* **2013**, *298*, 303.
31. Wongpanit, P.; Sanchavanakit, N.; Pavasant, P.; Bunaprasert, T.; Tabata, Y.; Rujiravanit, R. *Eur. Polym. J.* **2007**, *43*, 4123.
32. Huang, J.; Zou, J. W.; Chang, P. R.; Yu, J. H.; Dufresne, A. *eXPRESS Polym. Lett.* **2011**, *5*, 362.
33. Morin, A.; Dufresne, A. *Macromolecules* **2002**, *35*, 2190.
34. Nair, K. G.; Dufresne, A. *Biomacromolecules* **2003**, *4*, 657.
35. Ji, Y.; Wolfe, P. S.; Rodriguez, I. A.; Bowlin, G. L. *Carbohydr. Polym.* **2012**, *87*, 2313.
36. Knaul, J. Z.; Hudson, S. M.; Creber, K. A. M. *J. Appl. Polym. Sci.* **1999**, *72*, 1721.